Closed-form coherent Gaussian noise model applicable to arbitrary flexible grid and heterogeneous links

Fangyuan Zhang, Alex W. MacKay
Ciena Corporation, 383 Terry Fox Dr., Ottawa, Ontario, Canada, K2K 0L1
Author email-address: fzhang@ciena.com

Abstract: A closed-form expression of the coherent contribution of Gaussian noise nonlinear interference is presented. This model shows good agreement with a complete Gaussian noise model and a split-step model and applies in arbitrary link configurations.

1. Introduction

The ability to quickly and accurately model nonlinear interference (NLI) is important for various applications in optical network planning, design, and operation such as route viability determination and performance optimization. Over the past several years, different variants of Gaussian noise (GN) models have become popular tools to estimate NLI in optical networks [1-8]. There are numerous popular variants with varying complexity and accuracy which consider different physical effects or system variations. One feature which is missing from popular variants is a closed-form method to compute coherent NLI in an arbitrary heterogeneous link where each span may have different physical properties. In many cases it is reasonable to ignore this impact because it is much smaller than the incoherent NLI contribution per span, but after many spans have been traversed, ignoring this effect can lead to underestimation of total NLI and therefore optimistic quality of transmission (QoT) estimation. This effect is especially important in long terrestrial and backbone routes where there are often varying fiber types and characteristics along the link. Another common assumption to simplify integration is to assume moderately high span loss, where the nonlinearity ends up underestimated in low loss spans. In [7], this is addressed, but only in the Nyquist DWDM case. In this paper, we propose and demonstrate a closed-form expression for a coherent GN model (CF CGN) which can be applied to heterogeneous links with arbitrary spectral profiles, with spans of arbitrary loss.

2. Mathematical expression of the closed-form coherent GN model

The nonlinear noise-to-signal ratio (NSR_{NL}) computed by the GN model, can conveniently be separated into two parts:

$$NSR_{NL,n}(N_s) = NSR_{NL,n}^{IC}(N_s) + NSR_{NL,n}^{cc}(N_s) \tag{1}$$

where $NSR_{NL,n}^{IC}(N_s)$ is the incoherent contribution (IC) of NLI generated on the n^{th} channel due to the N_s spans in the path, and $NSR_{NL,n}^{cc}(N_s)$ is the coherent contribution (CC) of NLI generated on the n^{th} channel due to all spans between first and N_s^{th} span in the path [1]. For $NSR_{NL,n}^{IC}$ (Eq. (2)), we include self-channel interference (SCI) and cross phase modulation (XPM), and neglect other cross-terms including four-wave mixing (FWM). The SCI derivation directly follows [7], while the XPM part follows a similar derivation to Eq. (40) in [1] without the high loss approximation, and considers frequency-dependent γ and β, in both cases using rectangular integration surfaces over channels:

$$NSR_{NL,n}^{IC}(N_s) = \sum_{k=1}^{N_s}\sum_{m=1,m\neq n}^{N_{ch}} 4\gamma_m^2(k)A_{eq,m}^2(k)P_m^2(k)/(27\pi a_{eq,m}(k)\beta_{2,mn}(k)B_{ch,m}^2)$$
$$\left\{\text{asinh}\left(\frac{\pi^2\beta_{2,mn}(k)B_{ch,m}}{2a_{eq,m}(k)}\left[(f_m-f_n)+\frac{B_{ch,m}}{2}\right]\right)-\text{asinh}\left(\frac{\pi^2\beta_{2,mn}(k)B_{ch,m}}{2a_{eq,m}(k)}\left[(f_m-f_n)-\frac{B_{ch,m}}{2}\right]\right)\right\}+(4\gamma_n^2(k)A_{eq,n}^2(k)P_n^2(k)/$$
$$27\pi a_{eq,n}(k)\beta_{2,n}(k)B_{ch,n}^2)\,\text{asinh}\left(\pi^2\beta_{2,n}(k)B_{ch,n}^2/4a_{eq,n}(k)\right) \tag{2}$$

$$A_{eq,n}(k) = \left(1-e^{-\alpha_n(k)L(k)}\right)^2/(1-e^{-\alpha_n(k)L(k)}-\alpha_n(k)L(k)e^{-\alpha_n(k)L(k)}) \tag{2.1}$$

$$a_{eq,n}(k) = \alpha_n(k)/2 * \left(1-e^{-\alpha_n(k)L(k)}\right)/(1-e^{-\alpha_n(k)L(k)}-\alpha_n(k)L(k)e^{-\alpha_n(k)L(k)}) \tag{2.2}$$

where *m* and *n* index channels, N_{ch} is the total number of channels and k indexes spans. P is launch power into a span, B_{ch} and f are channel bandwidth and center frequency, L is span length, γ is nonlinear coefficient, α is power attenuation coefficient, β_2 is second order dispersion coefficient, and $\beta_{2,mn}$ is the average β_2 of channel *m* and *n*.

For $NSR_{NL,n}^{CC}$, we start from Eq. (100) in [8] and only consider the SCI as it is dominant part of the NLI CC. We derive an equivalent form representing the multi-span NLI power spectral density (PSD) at the end of the N_S^{th} fiber, which only considers SCI and arrive at the following relation for channel *n*:

$$G_{NLI,n}(f) = \frac{16}{27}\iint_{-\infty}^{\infty} g_n(f_1)g_n(f_2)g_n(f_1+f_2-f)H_{N_s}(f_1,f_2,f)\,df_1df_2 \tag{3}$$

$$H_{N_s}(f_1,f_2,f) = \left|\sum_{k=1}^{N_s} \gamma_n(k)P_n(k)\sqrt{P_n{}'(N_s)}\exp\left[j\phi_k(f_1,f_2,f)\right] \times \xi_k(f_1,f_2,f)\right|^2 \tag{3.1}$$

$$\phi_k(f_1,f_2,f) = 4\pi^2(f_1-f)(f_2-f)\sum_{l=1}^{k-1}\beta_{2,n}(l)L_s(l) \tag{3.2}$$

$$\xi_k(f_1,f_2,f) = \frac{1-\exp(-\alpha_n(k)L_n(k))\exp\left(j4\pi^2(f_1-f)(f_2-f)\beta_{2,n}(k)L_s(k)\right)}{\alpha_n(k)-j4\pi^2(f_1-f)(f_2-f)\beta_{2,n}(k)} \tag{3.3}$$

where $\phi_k(f_1,f_2,f)$ is the accumulated walk-off effect from the beginning of link to the beginning of k^{th} span, i.e., $\phi_1(f_1,f_2,f)=0$, $g_n(f)$ is the normalized PSD for the probe channel [9], $\xi_k(f_1,f_2,f)$ is four-wave-mixing efficiency of the k^{th} span, and $P'_n(N_s)$ is the probe channel power at the end of N_s^{th} span.

If we approximate the angle of the four-wave mixing term across spans (Eq. (4.1)) to be the same, as is the case for moderately high dispersion spans, we can rewrite the NLI contribution of N_s^{th} span only as:

$$H_{N_s}(f_1,f_2,f) - H_{N_s-1}(f_1,f_2,f) = 2\left|A_{N_s}(f_1,f_2,f)\right|\sum_{k=1}^{N_s-1}\left|A_{n_s}(f_1,f_2,f)\right|\cos\left[\phi_{N_s}(f_1,f_2,f)-\phi_k(f_1,f_2,f)\right] + \left|A_{N_s}(f_1+f_2-f)\right|^2 \tag{4}$$

$$A_k(f_1,f_2,f) = \gamma_n(k)P_n(k)\sqrt{P_n{}'(N_s)}\xi_k(f_1,f_2,f) \tag{4.1}$$

where the first term of Eq. (4) is the CC and second term is the SCI IC of N_s^{th} span which is considered in Eq. (2). To find the CC of NLI NSR of the N_s^{th} span which beats with all preceding spans, we only consider the first term of Eq. (4) and solve in Eq. (3), then divide by the probe channel PSD. To find the accumulated CC of all spans we sum the contributions of all spans. We assume that the channel spectrum is rectangular, and approximate the integral with an upper bound via the Cauchy-Shwarz inequality to arrive at the model for coherent NSR for all spans in the path:

$$NSR_{NL,n}^{CC}(N_s) = \begin{cases} \dfrac{16}{27}\displaystyle\sum_{N_s'=2}^{N_s}\gamma_n(N_s{}')L_{eff,n}(N_s{}')P_n(N_s{}')\sum_{k=1}^{N_s'-1}\frac{\gamma_n(k)L_{eff,n}(k)P_n(k)}{\pi\tau_{CD,n}(k,N_s')B_{ch,n}^2}, & N_s>1 \\ 0, & N_s=1 \end{cases} \tag{5}$$

$$\tau_{CD,n}(k,N_s) = \sum_{l=k}^{N_s-1}\beta_{2,n}(l)L(l) \tag{5.1}$$

where L_{eff} is the effective length. The CF CGN results from Eq. (2) and (5) into Eq. (1), providing the total NLI NSR.

3. Results

We first compare the CF CGN with the original, complete, homogeneous-span GN model (OGN), which is Eq. (G.3) of [8] using hexagonal channel integration surfaces and is solved by a Quasi-Monte Carlo integration which was tested for convergence. We compare our CF CGN model to the OGN on 20 spans non-dispersion shifted fiber (NDSF), enhanced large effective area fiber (ELEAF), and TrueWave Classic (TWC) with three different span lengths: 40 km, 80 km, and 120 km. The fiber parameters at 1550 nm are summarized in table 1 of [9] with a nonlinear refractive index of 2.64×10^{-20} m^2/W. The power profile is flat on each span with fixed power per signal: 3 dBm on NDSF, 1 dBm on ELEAF, 0 dBm on TWC, with 76 56.8 GBaud signals with 61.5 GHz channel spacing in the C-band. Fig. 1 shows good agreement in all cases, but there are some discrepancies due to approximations made.

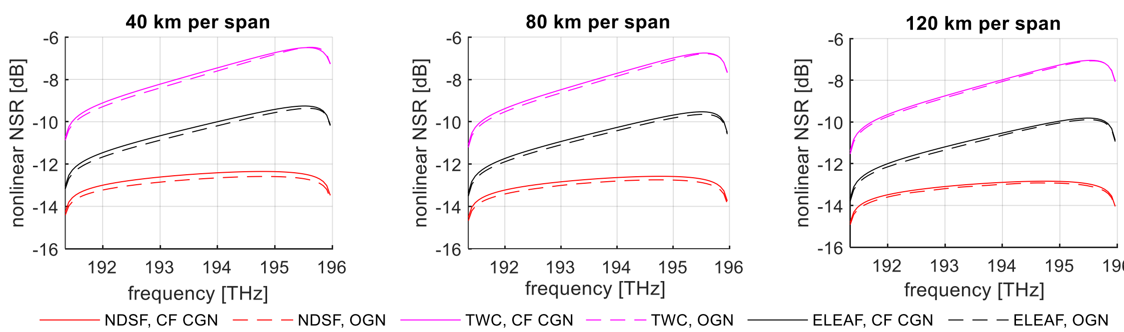

Fig. 1. Comparison of CF CGN with OGN in 20 span homogenous links with various fiber lengths and types

We next compare the CF CGN in a heterogenous link with a split-step Fourier method (SSFM) simulation using amplified spontaneous emission (ASE) channels since integrating a complete GN model is challenging in arbitrary, heterogeneous links. To generate a realistic link, we choose a random set of fiber types and lengths based on statistical distributions from a carrier network shown in Fig. 3 (a) and (b). The fiber order in the propagation model is: [3×NDSF, TWRS, NDSF, ELEAF, 2×NDSF, TWC, ELEAF, 2×NDSF, ELEAF, 15×NDSF, TWC, TWRS, 2×ELEAF, 4×NDSF, TWC, NDSF, 2×ELEAF]. The fiber parameters of TWRS (TrueWave Reduced Slope) fiber are the same as TWC except with 4.4 ps/nm/km dispersion and 0.215 dB/km attenuation at 1550 nm. The fiber lengths in order are [66, 74, 78, 130, 94, 119, 94, 65, 58, 84, 67, 73, 70, 101, 90, 105, 64, 70, 70, 90, 33, 98, 51, 25, 42, 63, 71, 30, 105, 80, 73, 122, 72, 64, 78, 61, 67, 104, 56, 65] km. The transmitted spectrum is 76 56.8 GHz wide, 61.5 GHz spaced ASE channels across the C-band, each shaped with a 1/14 roll-off factor root raised cosine. The per-channel launch powers into each span are [-2.6, -2, -1.8, -0.1, -0.6, -0.5, -0.6, -2.7, -6.5, -3, -2.5, -2.1, -4, -0.1, -0.9, 0.1, -2.7, -2.3, -2.3, -0.9, -4.9, -0.4, -3.6, -5.5, -4.3, -2.8, -2.2, -5.1, -3, -4, -3.8, -0.3, -2.2, -2.7, -1.8, -2.9, -5.8, 0.1, -5, -4.4] dBm. The NLI NSR are compared at lower, middle, and upper frequencies of the C-band in Fig. 2 for SSFM, CF CGN, and NLI of IC (CF IGN) of equation (2). In Fig. 2 we observe small errors between SSFM and CF CGN, while CF IGN can underestimate fiber nonlinearity by up to 0.8 dB at high span counts.

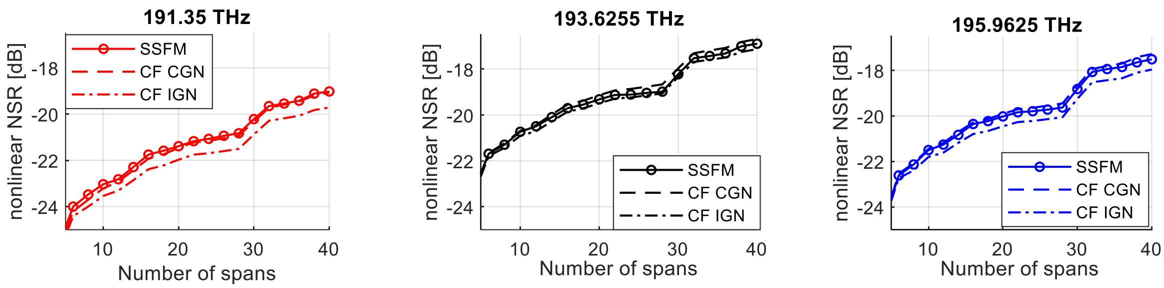

Fig. 2. Comparison of SSFM and CF CGN, CF IGN method in a heterogeneous link with random channel power

To show the alignment over a variety of cases, we then compared the CF CGN and CF IGN to SSFM under 154 different randomly generated heterogeneous 40 span scenarios, where we compared the error at spans two through 40 at 5 different probe frequencies, yielding $154 \cdot 39 \cdot 5 = 30030$ data points. The fiber length and type are chosen from the distributions in Fig 3 (a) and (b). The spectrum in each scenario are different combinations of 35 GHz wide ASE channels with 50 GHz spacing, 56.8 GHz channels with 61.5 GHz spacing, and 95 GHz wide channels with 102.5 GHz spacing. For each channel on each span, the launch power is configured to be at approximately the optimum launch based on an assumed downstream amplifier model, with ± 3 dB of random noise to generate shaped profiles. Fig. 3(c) shows the difference between the CF CGN and CF IGN relative to SSFM in all 30030 cases across channels and number of spans traversed. The mean, standard deviation, and mean square error (MSE) are -0.058 dB, 0.29 dB and 0.087 dB^2 respectively for CF CGN relative to SSFM and -0.50 dB, 0.32 dB, and 0.35 dB^2 respectively for CF IGN relative to SSFM.

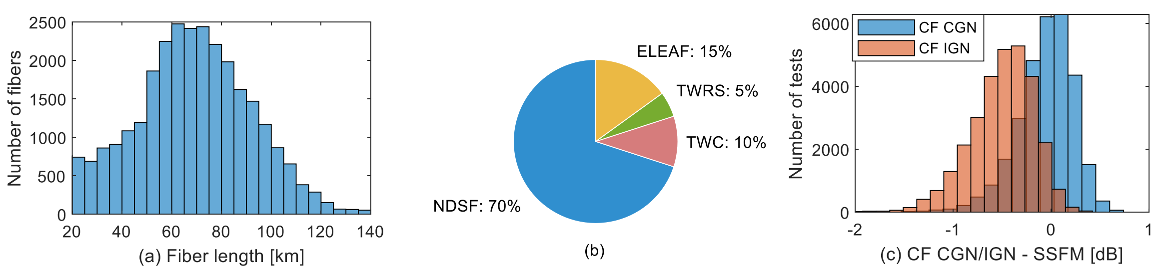

Fig. 3(a). Fiber length distribution, (b) Fiber type distribution, and (c) Distribution of simulated error of CF CGN and CF IGN vs SSFM

4. Conclusion

We proposed a closed-form coherent GN (CF CGN) model that is applicable to arbitrary spectral configurations, and heterogeneous link conditions which has good agreement with accurate GN model variants and SSFM models. The mean error and MSE of CF CGN relative to SSFM are -0.058 dB and 0.087 dB^2 respectively across many simulations ranging from 2 to 40 spans of propagation, whereas a GN model considering only incoherent NLI was shown to have a -0.50 dB mean error and 0.35 dB^2 MSE over the same simulations yielding optimistic NLI estimates. The CF CGN can therefore be considered for a fast NLI estimator considering coherent NLI.

References

[1]. P. Poggiolini, et al., JLT, 30(24), 3857-3879 (2012).
[2]. P. Poggiolini, et al., JLT,32(4), 694-721(2014).
[3]. P. Poggiolini, et al., arXiv:1209.0394 (2012).
[4]. H. Buglia, et al., JLT, doi: 10.1109/JLT.2023.3315127.
[5]. P. Poggiolini, et al., arXiv:1906.03883 (2019).
[6]. A. Carena, et al., OE, 22(13), 16335-16362 (2014).
[7]. M.R. Zefreh, et. al, arXiv:2111.04584 (2021).
[8]. P. Poggiolini, et al., arXiv:1209.0394 (2012).
[9]. F. Zhang, et al., JOCN, 9(4), C88-C97 (2017)